

Quantum entanglement of angular momentum states with quantum numbers up to 10,010

Robert Fickler^{a,b,c,1}, Geoff Campbell^d, Ben Buchler^d, Ping Koy Lam^d, and Anton Zeilinger^{a,b,1}

^aInstitute for Quantum Optics and Quantum Information, Austrian Academy of Sciences, 1090 Vienna, Austria; ^bFaculty of Physics, University of Vienna, 1090 Vienna, Austria; ^cMax Planck Centre for Extreme and Quantum Photonics, Department of Physics, University of Ottawa, Ottawa, ON, Canada K1N 6N5; and ^dCentre for Quantum Computation and Communication Technology, Research School of Physics & Engineering, Australian National University, Canberra, ACT 2601, Australia

Contributed by Anton Zeilinger, October 11, 2016 (sent for review July 2, 2016; reviewed by Fabio Sciarrino and Stephen P. Walborn)

Photons with a twisted phase front carry a quantized amount of orbital angular momentum (OAM) and have become important in various fields of optics, such as quantum and classical information science or optical tweezers. Because no upper limit on the OAM content per photon is known, they are also interesting systems to experimentally challenge quantum mechanical prediction for high quantum numbers. Here, we take advantage of a recently developed technique to imprint unprecedented high values of OAM, namely spiral phase mirrors, to generate photons with more than 10,000 quanta of OAM. Moreover, we demonstrate quantum entanglement between these large OAM quanta of one photon and the polarization of its partner photon. To our knowledge, this corresponds to entanglement with the largest quantum number that has been demonstrated in an experiment. The results may also open novel ways to couple single photons to massive objects, enhance angular resolution, and highlight OAM as a promising way to increase the information capacity of a single photon.

quantum entanglement | orbital angular momentum | photonic spatial modes | quantum foundations

Photonic systems are an excellent platform to test the foundations of quantum physics (1). Photonic technologies used to generate, manipulate, and measure one of its key features, quantum entanglement, have matured to an unprecedented level. In various experiments the limit of extending quantum mechanical predictions to the macroscopic regimes have been investigated by increasing the distance between the entangled photons (2, 3), the numbers of involved photonic systems (4), or the dimensionality of the entanglement (5). In another approach, the property of orbital angular momentum (OAM), which is related to the helical phase structure of the photons (6) in the paraxial regime and can be used to rotate particles around the optical axis (7), has been explored in quantum entanglement experiments (8). Interestingly, according to quantum theory this angular momentum can, in principle, be arbitrarily large even for entangled quantum states of single photons. If large enough, this angular momentum can conceivably be transferred to macroscopic particles, which could open novel ways of investigating light–matter interactions. Additionally, large OAM quanta of photonic quantum states are an interesting property to investigate the fundamental question regarding the existence of a quantum-classical transition. It is still believed by many people and often cited in textbooks in connection to Bohr’s correspondence principle (see e.g., ref. 9) that the quantum-classical transition has to occur when the quantum number of the investigated state becomes very large. However, in the opinion of the authors and many others, such a simple relation is not correct (e.g., see also ref. 10). Therefore, generating quantum states with large quantum numbers (e.g., high OAM values) are important experimental tests to challenge and clarify these fundamental questions. A recent experiment toward these directions demonstrated the entanglement of two photons with up to 300 quanta of OAM (11).

Here, we extend the experimental investigation of entanglement of high angular momenta and report the generation of entanglement

between polarization and more than 10^4 quanta of OAM. To generate this complex hybrid-entangled state, we start with bipartite polarization entanglement and transfer one photon’s polarization to a transverse spatial mode carrying 500, 1,000, or 10,010 quanta of OAM. We realize this transfer in a Michelson-type interferometric scheme, in which we insert spiral phase mirrors (SPMs) to imprint the high OAM quanta onto the photons. We test the generated entanglement in two different ways. First, we use an intensified CCD camera in a coincidence-imaging scheme to show entanglement between the polarization of one photon and its entangled partner that carries 500h of OAM. For entangled photons carrying up to 10,010h of OAM we replace the camera by an appropriate mask and again detect OAM superposition states in coincidence with the polarized partner photon. All of the results show clear signatures of quantum entanglement, which demonstrates that OAM quantum numbers of single photons can exceed 10,000 and still be entangled to its partner photon’s polarization.

Single photons in a transverse spatial mode with a helical phase front $e^{il\theta}$ (l being an integer value) contain, in the paraxial limit, l quanta of OAM with respect to optical axis (6). Such phase structures are also often described by their topological charge, namely how many twists the phase of light undergoes in one wavelength. Light exhibiting this twisted phase distribution has a phase singularity (i.e., optical vortex) for $l \neq 0$ in the center of the mode, which leads to a null intensity along the beam axis. Consequently, such modes are often called “doughnut modes” and have become important for various applications in quantum and also in classical experiments (12). There are different techniques to generate such phase structures, among which computer-generated holograms

Significance

Challenging quantum mechanical predictions is an important task to better understand the underlying principles of nature and possibly develop novel applications. Quantum entanglement as one of the key features is often investigated in optical experiments to push the known limits from smaller to larger scales, for example by increasing the number of entangled systems, their separation, or dimensionality. In the present study we pursue another route and investigate photons with large quantum numbers. We demonstrate entanglement between a photon with orbital angular momentum quantum numbers up to 10,010 and its partner encoded in polarization. The results show how complex the structure of entangled photons can be and hint at the large information content a single quantum system is able to carry.

Author contributions: R.F., P.K.L., and A.Z. designed research; R.F. performed research; G.C., B.B., and P.K.L. fabricated spiral phase mirrors; R.F. and A.Z. analyzed data; and R.F., G.C., B.B., P.K.L., and A.Z. wrote the paper.

Reviewers: F.S., Università Sapienza; and S.P.W., Federal University of Rio de Janeiro.

The authors declare no conflict of interest.

¹To whom correspondence may be addressed. Email: rfickler@uottawa.ca or anton.zeilinger@univie.ac.at.

This article contains supporting information online at www.pnas.org/lookup/suppl/doi:10.1073/pnas.1616889113/-DCSupplemental.

(13), spiral phase plates (14), spatial light modulators (15), or specialized liquid crystal devices, so-called q-plates (16), have attracted much attention.

Recently, a technique was established that is able to imprint unprecedented high quanta of OAM onto light (17, 18). Here, the required spiral phase structure is mapped onto the surface profile of a mirror, hence the name SPM. To realize the required phase modulation the surface structure needs to have an azimuthal depth dependence $d(\phi) = l\phi\lambda/(4\pi)$, where $l \in \mathbb{Z}^+$, $\phi \in [0, 2\pi)$ is the azimuthal angle, and λ corresponds to the wavelength of the photons. If photons are reflected from the surface they experience an azimuthal path difference of $2d(\phi)$, which in turn leads to a spiral phase of $\theta = 2d(\phi)/\lambda$. Thus, the imprinted azimuthally varying phase front corresponds to l multiples of 2π and thus l quanta of OAM. The SPMs are produced by direct machining of the surface of an aluminum disk (2-in. diameter) with an ultra-precision single-point diamond turning lathe (Nanotech 250UPL). For large values of l a steep discontinuity would appear at $\phi = 0^\circ$, which would be an impractical surface to machine. Instead, the surface is divided into n angular segments, each imprinting the n th part of the required spiral phase ramp. We are using three different SPMs in our experiments that are fabricated with 25, 25, and 125 segments, each imprinting an azimuthal phase ramp of 40π , 80π , or 160π (see Fig. 1, *Lower Right*). Hence, photons that are reflected from these SPMs have a spiral phase front corresponding to 500h, 1,000h, or 10,000h of OAM, respectively. Unlike pixelated programmable spatial light modulators, the efficiency of mode conversion from a fundamental Gauss mode to an OAM-carrying vortex mode using SPMs is close to that given by the reflectivity of aluminum, provided the machining is perfect and the numerical aperture of the optics is sufficiently large to capture all of the reflected light. With this technique it is possible to shape the wave front of the light with a higher accuracy and generate photons with larger quantum numbers than with any commercially available devices.

The ability to efficiently produce very-high-order vortex modes enabled us to test whether such high angular momentum quantum numbers can experimentally be imprinted onto light. More importantly, we are able to investigate whether single photons carrying high OAM quanta can be entangled with a partner photon's degree of freedom, thereby generating quantum states with unprecedented large quantum numbers. The general idea, similar to experiments reported earlier (11, 19–22), is to start with polarization entanglement, send one photon in its unchanged polarization state to Alice, and transfer Bob's photon to the OAM degree of freedom while maintaining the entanglement (Fig. 2). The transfer of Bob's photon to a mode with high OAM quanta is realized in a

Michelson-type interferometer where the photon's path is split dependent on its polarization. Then, the photon's transverse spatial phase profile is modulated by the SPMs to have the high-order helical structure exhibiting a large OAM quantum number. Afterward, the paths are recombined and the polarization information is erased by a polarizer at 45° . Hence, the created hybrid-entangled biphoton state shared between Alice and Bob reads as follows:

$$|\psi\rangle = a|H\rangle|+l\rangle + e^{i\varphi}b|V\rangle|-l\rangle, \quad [1]$$

where a , b , and φ are real ($a^2 + b^2 = 1$), l stands for the quanta of OAM, H (V) corresponds to horizontal (vertical) polarization, and the positions of the ket-vectors label Alice's and Bob's photon, respectively. To verify the generated entanglement, we take advantage of a specific feature of the superposition structure of the equally weighted OAM superposition states $|+l\rangle + e^{i\varphi}|-l\rangle$. The intensity pattern shows a petal-wheel-like pattern of $2l$ maxima in a ring (Fig. 1). The orientation γ of the pattern is directly linked to the phase ϑ via $\gamma = [\vartheta/(2l)] * [360^\circ/(2\pi)]$. Thus, a precise measurement of the petal-wheel structure or the angular probability distribution of Bob's photons can be directly used to distinguish different superpositions. In combination with the coincident measurement of the polarization of Alice's photon, these measurements can be used to test for entanglement.

Results

In a first series of experiments we test the Michelson-type interferometric transfer setup with a diagonally polarized laser (810-nm wavelength) and show that the SPMs are indeed able to generate light fields with unprecedented quanta of OAM. Note that we also refer to quanta of OAM in the following first experiment that only involve light from a laser although it might be perfectly described in the classical Maxwell-theory of light and large topological charges. However, we demonstrate in the experiments investigating quantum entanglement afterward that the description with quantum numbers or quanta of OAM is fully justified.

We start by transferring photons from a Gaussian mode with a beam diameter of around 1 in. to a mode with 500 or 1,000 quanta of OAM. Typical conversion efficiencies, that is, percentages of light transferred from the Gaussian mode to OAM carrying light modes, significantly larger than 50% are observed. This becomes apparent in Fig. 1 due to no visible intensity along the optical axis. In both cases the complex superposition structure formed by $2l$ maxima, which were counted directly from the recordings, agrees exactly with the expected values (Fig. 1 *A* and *B*). The maxima were counted by a computer program after contrast enhancement.

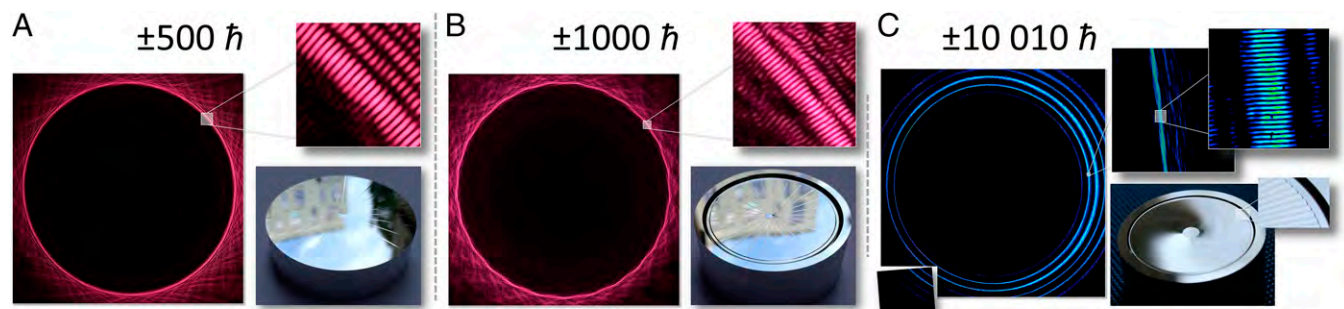


Fig. 1. Demonstration of high-order OAM mode generation with SPMs and an intense laser. Modes are generated by a diagonally polarized laser (~ 0.5 mW) sending through the transfer setups with SPMs for 500h (*A*), 1,000h (*B*), and 10,000h (*C*). Images were taken with a single-lens reflex camera (*A* and *B*, beam diameter around 15 mm) or by stitching 20 images from a CCD camera together (*C*, beam diameter around 25 mm). A zoom reveals the typical superposition structure from which the OAM content can be deduced. Because we only modulate the phase of the light, higher-order radial modes with the same OAM content can be found in all images. On lower right sides, photos from the used SPMs are shown, which are made out of 2-in. aluminum plates. The required helical phase structure is realized by 25 (*A*), 25 (*B*), or 125 (*C*) segments (visible in all photos, especially in the zoomed inset in *C*), each modulating up to 40π , 80π , or 160π , respectively.

$$|H\rangle|+1000\rangle - |V\rangle|-1000\rangle$$

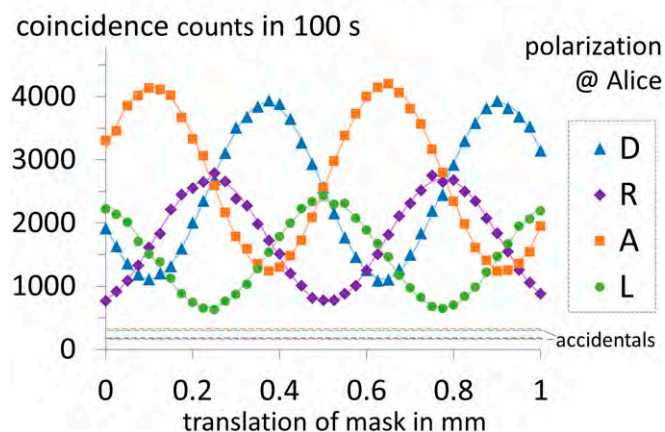


Fig. 4. Coincidence detections between Alice’s polarization measurements and Bob’s OAM measurements. The OAM photons were measured in different superposition states by detecting transmitted photons behind different positions of a slit mask that mimics the OAM superpositions structure. Because we only used 3% of the full mode and scanned fewer than two fringes, we approximated the circular rotation of 0.33° by a lateral translation. As expected for an entangled state, extrema of the opposing fringes belong to orthogonal polarizations and cannot be explained by a separable state. The corresponding entanglement witness verifies this observation by more than 10 SDs (Poissonian count statistics assumed; error bars are too small to be seen). Although unnecessary for the demonstration of entanglement, we also show the evaluated accidental coincidence detections (dashed lines) for the sake of completeness. For measurements in R/L-polarization bases the count rate was smaller, which stemmed from misalignments of the additional quarter wave plate.

approximation may be considered valid can be quantified using the paraxial estimator, \tilde{P} (24), which has a value of 1 in the limit of a perfectly paraxial beam. All our beams have a $\tilde{P} > 0.99999$. Thus, we are confident of the validity of the paraxial approximation in our experiments.

After having thus demonstrated the transfer classically, we show that an entangled quantum state with these high OAM quanta can be generated and measured. At first, we generate polarization entangled pairs by pumping a type-II down-conversion process (15-mm-long periodically poled KTP crystal) with a laser operating at 405 nm (~ 30 mW power) in a Sagnac-type arrangement (25, 26). For frequency and spatial filtering we implement a 3-nm bandpass filter and couple the generated photons into single mode fibers, after which we detect ~ 1.2 MHz of polarization entangled photon pairs with a wavelength of around 810 nm. Then, we transfer Bob's photon with the schemes described above to $\pm 500h$, $\pm 1,000h$, or $\pm 10,010h$ of OAM while keeping the entangled partner photon of Alice unchanged. To verify the successful generation of this state (1), we used two recently introduced methods, coincidence imaging (27) for ± 500 quanta and coincidence detection after masking (11) for $\pm 1,000$ or $\pm 10,010$ quanta.

In the first method we triggered an intensified CCD camera (ICCD; Andor iStar A-DH334T-18U-73, $\sim 20\%$ quantum efficiency, effective pixel size $13\text{ }\mu\text{m} \times 13\text{ }\mu\text{m}$, maximum 500-kHz triggering rate, 5-ns gating/coincidence window) to image in coincidence the transverse profile of the OAM photon at Bob's location. Here, the polarization measurement of Alice's photon, that is, the signal of a single photon avalanche photo diode (APD), serves as the trigger. Note that because of the intrinsic delay of the ICCD between the trigger detection and the actual gating of the ICCD, we delay the imaged photon by a 35-m-long fiber before it is transferred and recorded. The successful generation of the hybrid-entangled state (1) can be seen in Fig. 3, where the measurements of different

polarization superpositions trigger the camera to image different OAM mode superpositions and thus slightly rotated petal-wheel structures on the ICCD. To more quantitatively verify the non-separable nature of our measurements, we evaluate a witness that corresponds to the sum of the two visibilities in two mutually unbiased bases. Because separable states can only have a perfect visibility of 1 in one of these bases, the witness upper bounds the sum of the two visibilities to 1 for separable states. Values above this classical bound demonstrate quantum entanglement (27, 28). We measured accidental coincidences by shifting the delay of the trigger signal at the ICCD of around 100 ns and subtracted them from the count rates (see [Supporting Information](#) for more details). A witness value of 1.626 ± 0.022 (Poissonian counts statistics assumed) demonstrates a successful generation of quantum entanglement with $\pm 500h$ of OAM.

Although the coincidence imaging scheme works very well for SPMs imprinting 500 quanta of OAM, the low triggering rate and detection efficiency of the ICCD prevents its use for higher quantum numbers. Thus, for measurements of entanglement with $\pm 1.000h$ and $\pm 10.010h$ of OAM we measure the polarization of the

$$|H\rangle|+10010\rangle - |V\rangle|-10010\rangle$$

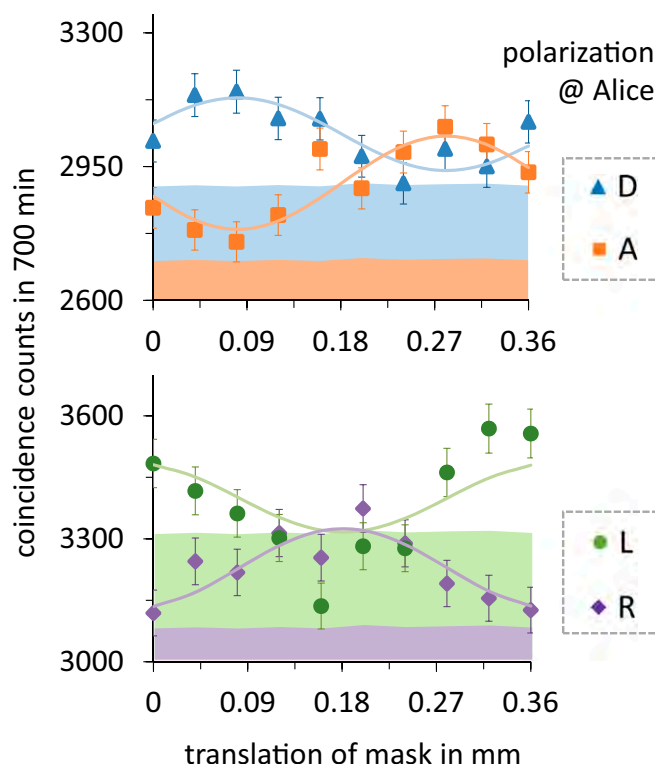


Fig. 5. Quantum entanglement between polarization and 10,010h of OAM. We recorded correlations in the coincidence counts between Alice’s polarization measurements and Bob’s OAM measurements of superposition states. Again, the OAM superpositions are measured by detecting transmitted photons behind a slit mask that mimics the superposition structure. The circular rotation of the mask ($<0.018^\circ$) is approximated by a linear translation. The colored region below each fringe corresponds to the accidental coincidence detections, derived from single counts and a measured coincidence window of 4.69 ± 0.34 ns. The error bars show Poissonian error estimation. The lines correspond to the best \sin^2 -fit function with the condition to be above the accidentals to have nonnegative coincidence rates. From the visibilities of the fitted functions we derived entanglement witness value above the classical bound.

unchanged photons of Alice in coincidence with the detections of Bob's transferred photons, which are transmitted through a mask that mimics the superposition pattern (11, 29). The ratio between slit width and the distance between the slits was $\sim 1/7$, which reduces the maximal measurable visibility to around 97%. Because the masks are fabricated with a low-precision laser cutter (resolution approximately 100 μm) and normal paper, we were only able to fabricate and use a small fraction of the whole slit mask (around 60 slits). This allowed us to approximate the curvature of slit arrangement by a linear distribution of slits over a $\sim 50\text{-mm}$ length. In a similar way we approximated the rotation of the mask during the measurements with a linear translation (Figs. 4 and 5). To fit the beam of photons to the dimensions of the mask, we had to enlarge the beam size with lenses and free propagation over many meters. The transmitted photons are detected by a bucket detector (APD, active area with a diameter of 500 μm) and recorded in coincidence with four polarization measurements of the partner photons (diagonal, antidiagonal, and left- and right-handed circular). From the shifted extrema of the four measured coincidence fringes the aforementioned entanglement witness can be evaluated.

For entanglement between polarization and 1,000 quanta of OAM we find a value of 1.128 ± 0.013 (Poissonian count statistics assumed) without any subtraction of background or accidental coincidences (Fig. 4), which verifies the nonseparable nature of the state. We note that if accidental coincidence detection are subtracted (procedure explained in more detail below) the witness value increases to 1.228 ± 0.013 .

As is visible in the laser images, the efficiency is drastically reduced for our final step, the generation and verification of entangled quantum states with 10,010 OAM quanta. Various sources of loss, such as the first transfer to ± 10 OAM quanta, the bright unused higher-order radial modes (Fig. 1C), the measurement of only 0.3% of the whole beam, and the lower detection efficiency when focusing on the bucket detector after the mask all lead to a coincidence rate that is more than 10 times smaller than the accidental coincidence detections (Fig. 5). Thus, subtraction of accidentals is indispensable. We evaluate them from the measured coincidence window of 4.68 ± 0.34 ns, which is in agreement with the one given by electronics of coincidence logic and single photon detections (*Supporting Information*). We test for signatures of quantum entanglement by evaluating the witness in two slightly different ways. In the first data analysis, we derive the required visibilities from fitting a \sin^2 -function, thereby taking into account all measured data points and increasing the statistical significance. For fitting we use a least-squares method including weighting of data points with respect to the errors and upper bounding the visibility to 1. We evaluate a witness value of 1.43 ± 0.25 , which exceeds the classical bound with 1.7 sigma significance. In a second method of analyzing the data we split the whole dataset into 10 equally long measurement intervals and evaluate for each the

witnesses separately. Again we correct for accidental coincidences by evaluating accidentals from single detections and only take values above the accidentals into account. Here, the mean value and the standard error of the mean over all 10 measured witnesses is found to be 1.41 ± 0.13 (see *Supporting Information* for more details, e.g., the 10 witness values).

Interestingly, both results show an even higher witness value than the measurements of 1,000h, which might be caused by the larger error margin. Because all results show values above the classical bound of 1, our findings can be seen as a clear signature that we successfully generated entanglement between polarization and up to 10,010 quanta of angular momentum.

Discussion

In summary, we took advantage of the abilities of recently developed SPMs to efficiently modulate light into wave fronts with very high complexity. We implemented the SPMs in an interferometric technique that enabled us to generate entanglement between polarization and up to 10,010 OAM quanta, thereby extending the measured amount of quanta per photon by two orders of magnitude. Because our findings demonstrate a quantum state with a very large quantum number, they can be viewed in the light of discussions about a possible quantum-classical transition for large quantum numbers. Along with the understanding of the authors, our results do not show a signature of such a transition and fully support the quantum mechanical description. Besides these fundamental aspects, the results could also be interesting for questions regarding the maximum capacity of information a single quantum carrier can possess. Although we only generated a two-dimensional state, the results are promising that the spatial degree of freedom of photons offers a very large state space to encode and manipulate quantum information. Similar reasoning also holds true for classical information technology. Moreover, it is known that certain applications such as angular sensing benefit in their sensitivity the larger the OAM quantum number is (11, 30). Here, applications where only low light intensities are allowed might especially benefit from the enhancement of large OAM values. Another possible advantage of very high quanta of OAM per single photon might be the enlarged transfer of momenta when light is interacting matter systems (e.g., the coupling of photons to massive objects in quantum optomechanical experiments) (31).

ACKNOWLEDGMENTS. R.F. thanks M. Krenn for fruitful and motivating discussions and acknowledges financial support by the Canada Excellence Chairs Program and Banting postdoctoral fellowship of the Natural Sciences and Engineering Research Council of Canada. This research was funded by the Austrian Academy of Sciences, European Research Council SIQS Grant 600645 EU-FP7-ICT, Austrian Science Fund SFB F40 (FOQUS), Australian Research Council Centre of Excellences Grant CE110001027, and Discovery Project Grant DP150101035. P.K.L. is also supported by Australian Research Council Laureate Fellowship FL150100019.

- Shadbolt P, Mathews JC, Laing A, O'Brien JL (2014) Testing foundations of quantum mechanics with photons. *Nat Phys* 10(4):278–286.
- Ursin R, et al. (2007) Entanglement-based quantum communication over 144 km. *Nat Phys* 3(7):481–486.
- Inagaki T, Matsuda N, Tadanaga O, Asobe M, Takesue H (2013) Entanglement distribution over 300 km of fiber. *Opt Express* 21(20):23241–23249.
- Yao XC, et al. (2012) Observation of eight-photon entanglement. *Nat Photonics* 6(4):225–228.
- Krenn M, et al. (2014) Generation and confirmation of a (100 x 100)-dimensional entangled quantum system. *Proc Natl Acad Sci USA* 111(17):6243–6247.
- Allen L, Beijersbergen MW, Spreeuw RJC, Woerdman JP (1992) Orbital angular momentum of light and the transformation of Laguerre-Gaussian laser modes. *Phys Rev A* 45(11):8185–8189.
- He H, Friese MEJ, Heckenberg NR, Rubinsztajn-Dunlop H (1995) Direct observation of transfer of angular momentum to absorptive particles from a laser beam with a phase singularity. *Phys Rev Lett* 75(5):826–829.
- Mair A, Vaziri A, Weihs G, Zeilinger A (2001) Entanglement of the orbital angular momentum states of photons. *Nature* 412(6844):313–316.
- Demtröder W (2010) *Atoms, Molecules, and Photons* (Springer, Heidelberg), 2nd Ed, p 194.
- Liboff RL (1975) Bohr correspondence principle for large quantum numbers. *Found Phys* 5(2):271–293.
- Fickler R, et al. (2012) Quantum entanglement of high angular momenta. *Science* 338(6107):640–643.
- Andrews DL, Babiker M, eds (2012) *The Angular Momentum of Light* (Cambridge Univ Press, Cambridge, UK).
- Heckenberg NR, McDuff R, Smith CP, White AG (1992) Generation of optical phase singularities by computer-generated holograms. *Opt Lett* 17(3):221–223.
- Beijersbergen MW, Coerwinkel RPC, Kristensen M, Woerdman JP (1994) Helical-wavefront laser beams produced with a spiral phaseplate. *Opt Commun* 112(5):321–327.
- Curtis JE, Koss BA, Grier DG (2002) Dynamic holographic optical tweezers. *Opt Commun* 207(1):169–175.
- Marrucci L, Manzo C, Paparo D (2006) Optical spin-to-orbital angular momentum conversion in inhomogeneous anisotropic media. *Phys Rev Lett* 96(16):163905.
- Campbell G, Hage B, Buchler B, Lam PK (2012) Generation of high-order optical vortices using directly machined spiral phase mirrors. *Appl Opt* 51(7):873–876.
- Shen Y, et al. (2013) Generation and interferometric analysis of high charge optical vortices. *J Opt* 15(4):044005.
- Żukowski M, Pykacz J (1988) Bell's theorem: Proposition of realizable experiment using linear momenta. *Phys Lett A* 127(1):1–4.

20. Nagali E, et al. (2009) Quantum information transfer from spin to orbital angular momentum of photons. *Phys Rev Lett* 103(1):013601.
21. Ramelow S, Ratschbacher L, Fedrizzi A, Langford NK, Zeilinger A (2009) Discrete tunable color entanglement. *Phys Rev Lett* 103(25):253601.
22. Galvez EJ, Nomoto S, Schubert W, Novenshtern M (2011) Polarization-spatial-mode entanglement of photon pairs. *International Conference on Quantum Information* (Optical Society of America, Washington, DC), p QMI18.
23. Siegman AE (1986) *Lasers* (University Science Books, Mill Valley, CA), Vol 37.
24. Vaveliuk P, Ruiz B, Lencina A (2007) Limits of the paraxial approximation in laser beams. *Opt Lett* 32(8):927–929.
25. Kim T, Fiorentino M, Wong FN (2006) Phase-stable source of polarization-entangled photons using a polarization Sagnac interferometer. *Phys Rev A* 73(1):012316.
26. Fedrizzi A, Herbst T, Poppe A, Jennewein T, Zeilinger A (2007) A wavelength-tunable fiber-coupled source of narrowband entangled photons. *Opt Express* 15(23): 15377–15386.
27. Fickler R, Krenn M, Lapkiewicz R, Ramelow S, Zeilinger A (2013) Real-time imaging of quantum entanglement. *Sci Rep* 3:1914.
28. Gühne O, Tóth G (2009) Entanglement detection. *Phys Rep* 474(1):1–75.
29. Krenn M, Handsteiner J, Fink M, Fickler R, Zeilinger A (2015) Twisted photon entanglement through turbulent air across Vienna. *Proc Natl Acad Sci USA* 112(46):14197–14201.
30. D'Ambrosio V, et al. (2013) Photonic polarization gears for ultra-sensitive angular measurements. *Nat Commun* 4:2432.
31. Aspelmeyer M, Kippenberg TJ, Marquardt F (2014) Cavity optomechanics. *Rev Mod Phys* 86(4):1391.